

## Effect of Boron in AHSS on Coatability in Hot-Dip Galvanizing

Daisuke Tahara<sup>†</sup>, Katsuya Hoshino, and Shoichiro Taira

*JFE Steel Corporation, 1 Kokan-cho, Fukuyama, Hiroshima, 721-8510, JAPAN*  
(Received February 08, 2024; Revised April 08, 2024; Accepted June 11, 2024)

Generally, Si and Mn are added to advanced high strength steel (AHSS) sheets. It is well known that these elements can form oxides during annealing and cause surface bare spots in hot-dip galvanizing due to their poor wettability with molten Zn. Boron (B) is also often added to AHSS to improve hardenability. However, few reports have investigated the effect of B on coatability, especially under low dew point conditions. To investigate the effect of B, B-free specimens and specimens containing 15 or 30 ppm B were prepared and annealed at low dew points from -60 to -45 °C. These specimens were dipped in a molten zinc. Their coatability was then evaluated based on the appearance. Results showed that the area of bare spots expanded as the B content increased and the dew point decreased. To understand the mechanism, annealed specimens without galvanizing were also prepared and analysed. XPS analysis showed that boron nitride (BN) was formed on the surface of B-added specimens. BN was considered to deteriorate coatability in hot-dip galvanizing because the estimated amount of BN increased as the B content increased and the dew point decreased, which showed the same trend as coatability.

**Keywords:** *B-added steel, Hot-dip galvanizing, Coatability, Dew point, Boron nitride*

---

### 1. Introduction

Demand for reduction of automotive body weight to decrease fuel consumption and greenhouse gas emissions has increased in recent years. To decrease body weight while maintaining collision safety, use of advanced high strength steel (AHSS) is expanding, and these steel sheets are also galvanized or galvanealed for corrosion resistance. AHSS often contains solute strengthening and hardening elements such as C, Si, Mn, P, B and Cr. However, it is well known that Si and Mn form oxides on the steel surface by selective oxidation in the annealing process. These oxides deteriorate coatability in hot-dip galvanizing due to their poor wettability and reactivity with molten Zn [1-3]. Therefore, various approaches to improve the coatability of AHSS have been demonstrated, such as controlling the dew point in the furnace of the continuous galvanizing line (CGL). For example, increasing the dew point results in formation of inner oxides and suppression of selective surface oxidation of Si and Mn because the oxygen potential in the furnace is increased [4,5]. Decreasing the dew point has also been investigated,

and this approach suppresses the velocity of selective oxidation of Si and Mn because the oxygen potential is decreased [6].

B is often added to AHSS to improve hardenability owing to its low cost and good performance with small addition. Several reports have investigated the coatability in hot-dip galvanizing of B-added steel annealed at high dew points such as -20 °C. For example, it was reported that B addition affects the morphology of oxides: Oxides become large and spherical because the melting point of Mn-B oxide is lower than that of Mn oxide [7]. It was also reported that B addition increases selective oxidation of Si and Mn [8,9]. From these results, B was considered to deteriorate coatability at high dew points. However, few reports have investigated the effect of B when the steel was annealed at a low dew point. Therefore, in this study, the effect of B on coatability at low dew points was investigated in terms of selective oxidation, oxide morphology and the surface segregation behaviour of B.

### 2. Experimental Procedure

#### 2.1 Test specimens

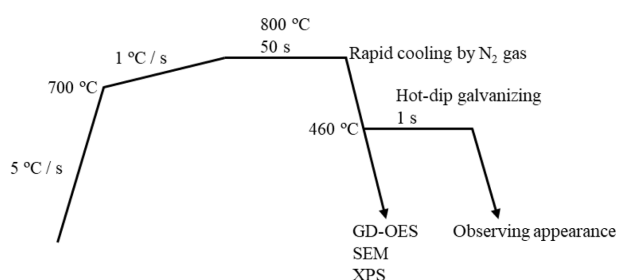
In order to investigate the effect of B, B-free specimens

---

<sup>†</sup>Corresponding author: [da-tahara@jfe-steel.co.jp](mailto:da-tahara@jfe-steel.co.jp)

**Table 1. Chemical composition of specimens (mass %)**

	C	Si	Mn	P	S	B
Steel 1 (B free)	0.08	0.2	3.0	0.005	0.001	Tr.
Steel 2 (15 ppm B)	0.008	0.2	3.0	0.005	0.001	0.0015
Steel 3 (30 ppm B)	0.08	0.2	3.0	0.005	0.001	0.0030

**Fig. 1. Schematic of annealing conditions**

and specimens containing 15 or 30 ppm B were prepared. The chemical composition of the specimens is shown in Table 1. The specimens used in this work were cast as 75 kg ingots in the laboratory. The ingots were then cut into blocks, reheated at 1250 °C for 1 hour, and hot rolled to a 30 mm thickness. Subsequently, the 30 mm thick plates were reheated again at 1250 °C for 1 hour and hot rolled to a 6 mm thickness. The plates were ground on both sides to a 2.5 mm thickness, annealed at 550 °C for 10 minutes, and pickled in a 5 vol% HCl solution at 80 °C. Finally, the plates were cold rolled to a thickness of 1.2 mm.

## 2.2 Annealing and hot-dip galvanizing

The specimens after cold rolling were cut to 70 × 180 mm and then annealed and hot-dip galvanized in a hot-dip process simulator (Rhesca). The annealing process was carried out in the infrared heating furnace of the simulator. The atmosphere of the furnace was 10 vol% H<sub>2</sub>-N<sub>2</sub> gas. The dew point of the furnace was also controlled to -60, -50 or -45 °C. Fig. 1 shows the temperature and treatment time used as annealing conditions in this experiment. After annealing, the specimens were cooled to 460 °C by N<sub>2</sub> gas and dipped in a molten zinc bath. Coatability was evaluated by the appearance of the galvanized specimens. Specimens without galvanizing were also prepared and analysed by the methods described below.

## 2.3 Surface observation and analysis

Depth profiles of the elemental composition were obtained by glow discharge optical emission spectrometry (GD-OES). The specimens were sputtered with Ar plasma, and the analysed spot was 4 mm Φ. The measuring time was 150 s with an interval of 0.1 s.

The surface of the annealed specimens was observed with a scanning electron microscope (SEM). The acceleration voltage in this observation was controlled to 1 kV. The oxide morphology and the difference of the chemical composition were observed with secondary electron (SE) images and energy selective backscattered electron (EsB) images, respectively.

The surface chemical composition of the annealed specimens was analysed by an X-ray photoelectron spectroscopy (XPS). A monochromatic Al K $\alpha$  anode, take-off angle of 45° and analysis area of 1  $\mu\text{m}^2$  were employed in the analysis. The spectra obtained in a narrow scan were quantified by peak fitting for all the elements detected in a wide scan.

## 3. Results and Discussion

### 3.1 Coatability in hot-dip galvanizing

Fig. 2 shows the appearance of the specimens after annealing and hot-dip galvanizing. Fig. 2a shows the results of the B-free specimens and specimens containing 15 and 30 ppm B annealed at the dew point of -50 °C. Only small bare spots were observed in the B-free specimen. These small bare spots have often been observed when AHSS was hot-dip galvanized due to selective oxidation of Si and Mn. On the other hand, large bare spots were observed on the specimens containing 15 and 30 ppm B, and the area increased at the higher B content. These results suggest that coatability in hot-dip galvanizing was deteriorated by B addition. Fig. 2b shows the specimens containing 15 ppm B which were annealed at the dew points of -60, -50 and -45 °C. In the case of

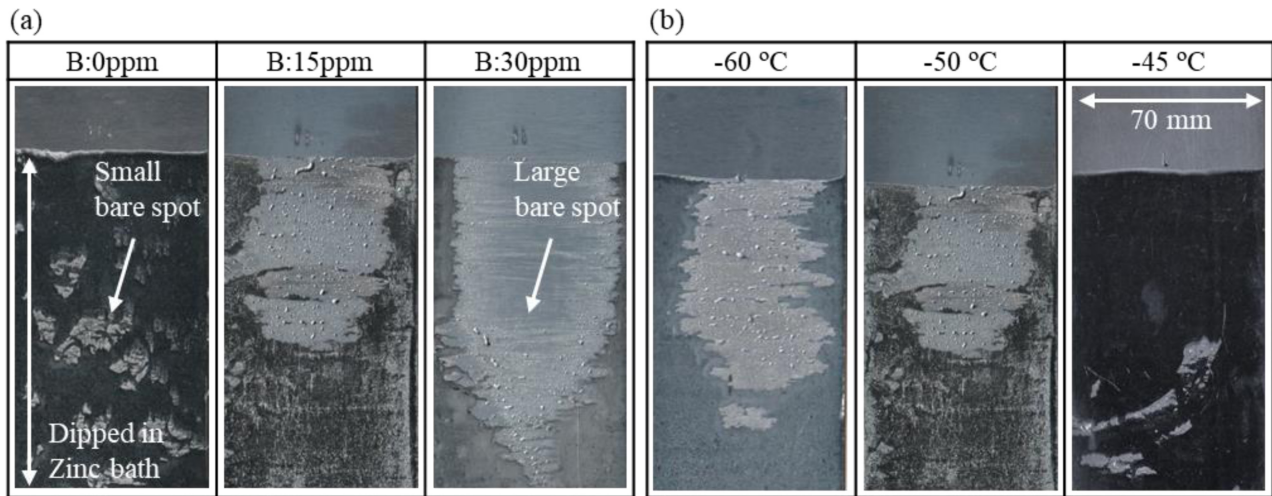


Fig. 2. Appearance of specimens after annealing and hot-dip galvanizing. (a) Dew point:  $-50\text{ }^{\circ}\text{C}$ , (b) 15 ppm B addition

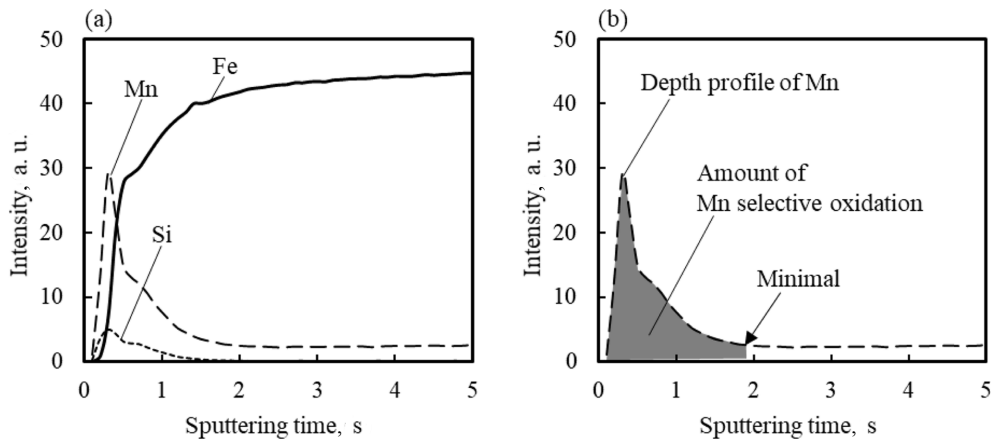


Fig. 3. (a) GDS depth profiles of specimen containing 15 ppm B annealed at dew point of  $-50\text{ }^{\circ}\text{C}$  (b) Definition of calculation of amount of selective oxidation

annealing at  $-45\text{ }^{\circ}\text{C}$ , large bare spots were not observed even though the specimen contained B. However, when the dew point was less than  $-50\text{ }^{\circ}\text{C}$ , a large bare spot was observed. Furthermore, the bare spot became larger when the dew point was  $-60\text{ }^{\circ}\text{C}$ . Therefore, these results suggest that the deterioration of coatability by B addition occurs only when the steel is annealed at a low dew point.

### 3.2 Selective oxidation of Si and Mn on surface

In order to evaluate the amount of selective surface oxidation, depth profiles were obtained by GD-OES. Fig. 3a shows the depth profiles of the specimens containing 15 ppm B annealed at  $-50\text{ }^{\circ}\text{C}$ . Peaks of both Si and Mn were observed within 1 s of sputtering time. This suggests that selective oxidation of Si and Mn on the surface is

caused by annealing. Therefore, in order to investigate the effect of selective oxidation on coatability, the amounts of selective oxidation were calculated by integrating the intensity from the steel surface to the point of the minimal value, as shown in Fig. 3b.

Fig. 4a shows the relationship between the B content and the amount of selective oxidation calculated by the method mentioned above. Firstly, selective oxidation of Si slightly decreased as the B content increased. Secondly, selective oxidation of Mn increased when 15 ppm B was added, but the amount of oxidation did not change when B addition was increased from 15 to 30 ppm B. These results suggest that selective oxidation of Si and Mn were not clearly promoted by B addition, and the large bare spot that occurred in hot-dip galvanizing was not related

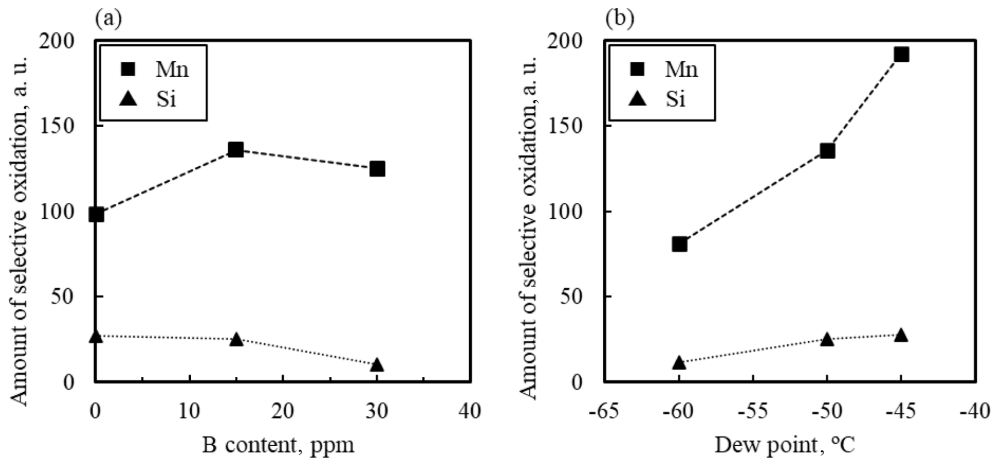


Fig. 4. Effects of (a) B content and (b) dew point on amount of selective oxidation of Mn and Si

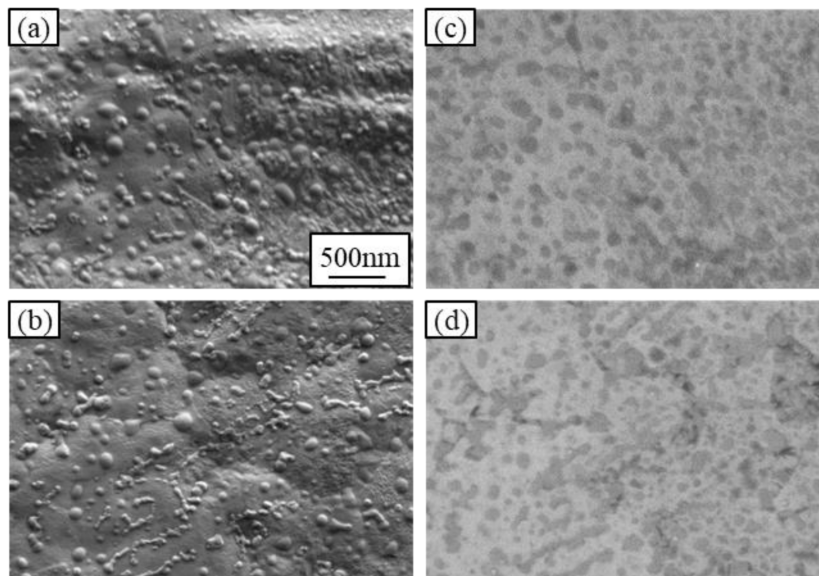


Fig. 5. SEM images of surface after annealing at dew point of  $-60\text{ }^{\circ}\text{C}$ ; (a) SE2 of B-free, (b) SE2 of 15 ppm B, (c) EsB of B-free and (d) EsB of 15 ppm B specimens

to the amount of selective oxidation. Fig. 4b shows the relationship between the dew point and the amount of selective oxidation. Selective oxidation of both Mn and Si increases as the dew point increases. This tendency can be understood as the result of an increase in the oxygen potential. However, this tendency is inconsistent with the result that bare spots were expanded by decreasing the dew point. Therefore, these results also suggest that the large bare spot that occurred in hot-dip galvanizing cannot be explained by the amount of selective oxidation of Mn and Si during annealing.

### 3.3 Observation of oxides formed on surface

Fig. 5 shows the results of SEM observation of the B-free specimen and the specimen containing 15 ppm B. Fig. 5a and b show SE images, i.e., the morphology of the surface. The results show that the morphology of the oxides was not changed by B addition. Fig. 5c and d are EsB images showing the difference of the chemical composition as contrast. The EsB images were almost the same in spite of the difference in the B content. In the results of energy dispersive X-ray spectroscopy (EDX), the areas of light contrast are the steel substrate and the areas of dark contrast are oxides of Si and Mn. Therefore,

the morphology and distribution of oxides on the surface were not different in the B-free and B-added specimens, meaning the deterioration of coatability shown in Fig. 2 also cannot be explained by the morphology and distribution of oxides formed during annealing.

### 3.4 Identification of boron on surface

In order to identify B on the surface, an XPS analysis was carried out. Fig. 6 shows the XPS wide spectrum of the B-free and 15 ppm B specimens annealed at the dew point of  $-50^{\circ}\text{C}$ . Most of the detected peaks were the same in the B-free and 15 ppm B specimens. However, the specimen containing 15 ppm B had a clear B1s peak (near 190 eV) and N1s peak (near 400 eV). Fig. 7 shows the narrow spectra of B1s and N1s of the same specimens as in Fig. 6. The binding energy of the B1s spectrum was about 191.3 eV, while that of N1s was about 398.5 eV. In addition, the quantities of B and N was calculated by peak fitting for all elements. As results, 7.6 at.% of B and 6.6

at.% of N were detected in the quantitative analysis, suggesting that BN was formed on the surface of the annealed specimen containing 15 ppm B because the binding energy was close to that of BN [10] and the quantities of B and N were almost equal.

Fig. 8a shows the amounts of B and N calculated from the results of the XPS analysis as a function of the B content of the steel. The results show that the amount of

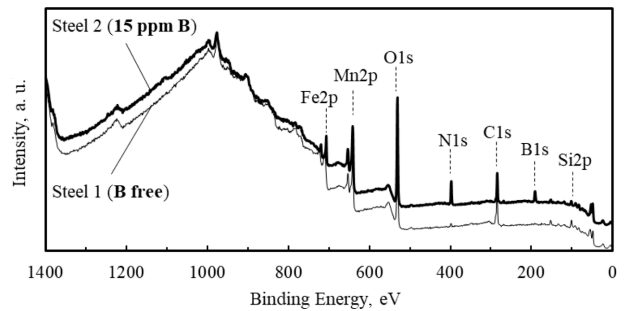


Fig. 6. XPS wide spectrum of specimens annealed at dew point of  $-50^{\circ}\text{C}$

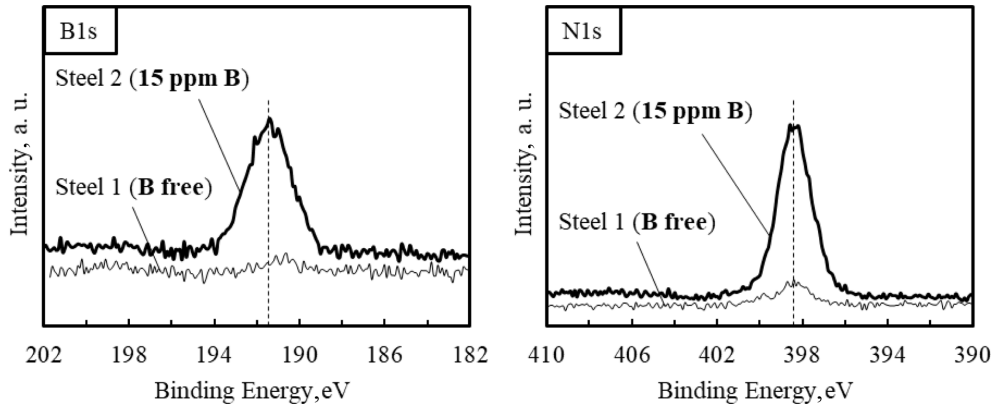


Fig. 7. B1s and N1s spectra of specimens annealed at dew point of  $-50^{\circ}\text{C}$

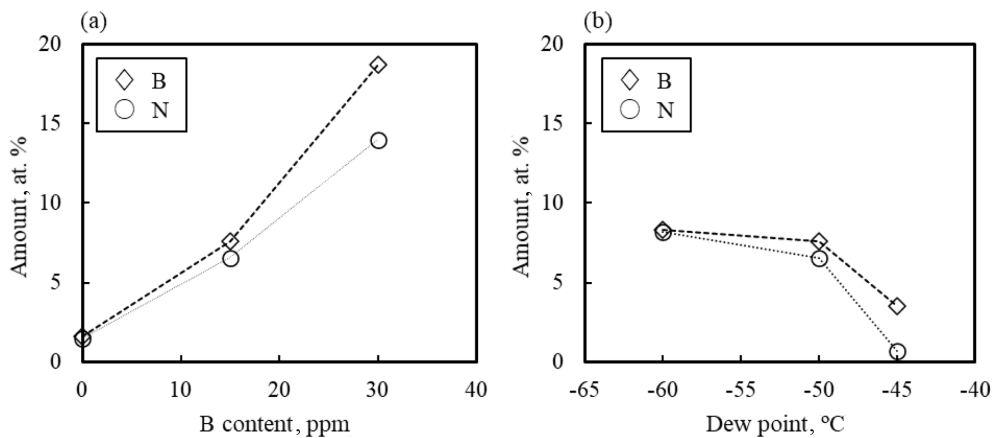


Fig. 8. Effects of (a) B content and (b) dew point on amounts of B and N

B and N increases as the B content increases. This tendency corresponds to the occurrence of the large bare spot in hot-dip galvanizing observed in the B-added specimens, as shown in Fig. 2a. Fig. 8b shows the amounts of B and N as a function of the dew point of annealing. The results show that the amount of B and N decreased as dew point increased, and at  $-45\text{ }^{\circ}\text{C}$ , little BN was formed. These results also correspond to the result that the large bare spots were observed at less than  $-50\text{ }^{\circ}\text{C}$ , as shown in Fig. 2b. These facts suggest that the large bare spot in hot-dip galvanizing shown in Fig. 2 could be caused by BN.

### 3.5 Estimated mechanism of effect of B on coatability in hot-dip galvanizing

The estimated mechanism by which B in the steel substrate affects hot-dip galvanizing, as described above, is shown in Fig. 9. In the case of B-free steel, small bare spots were caused by selective oxidation of Si and Mn. Although small bare spots were also occurred as a result of selective oxidation when B-added steel was annealed at  $-45\text{ }^{\circ}\text{C}$ , when B-added steel was annealed at less than  $-50\text{ }^{\circ}\text{C}$ , a large bare spot occurred because BN was formed in addition to the oxides of Si and Mn.

The formed BN may cover only the outermost surface

of annealed specimens because the analysis depth of XPS is several nanometres. Even though the amount of BN is small and its thickness is very thin, it can deteriorate wettability and reactivity with molten zinc more drastically than oxides, causing the large bare spot shown in Fig. 2, because it is well known that BN can hardly react with liquid metals due to its firm covalent bonding.

Regarding the formation of BN, some reports have mentioned that BN was formed by annealing at a low dew point under  $-50\text{ }^{\circ}\text{C}$  [11,12]. BN formation has also been predicted by an equilibrium calculation [13]. These reports mentioned that BN is more stable than oxides of B when the oxygen potential of the atmosphere is low and its nitrogen potential is high. In this study, BN was detected in the case of the B-added specimens annealed at the dew points of  $-50$  and  $-60\text{ }^{\circ}\text{C}$  in  $\text{N}_2$  gas, as shown in Fig. 8. However, BN did not form on the specimens containing B when annealed at the dew point of  $-45\text{ }^{\circ}\text{C}$ . These phenomena are close to those in the previous reports.

## 4. Conclusions

The effect of B on coatability in hot-dip galvanizing of steel sheets annealed at low dew points was investigated,

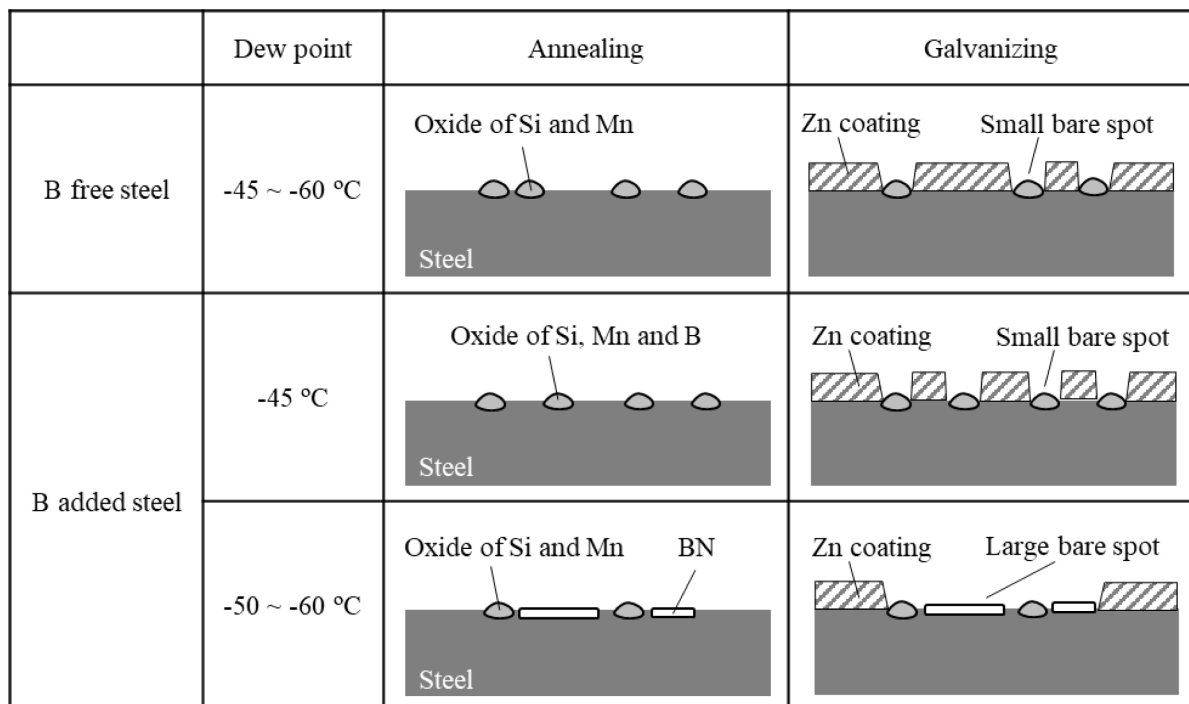


Fig. 9. Schematic images of estimated mechanism of effect of B on coatability in hot-dip galvanizing

and the following conclusions were obtained.

A large bare spot tended to occur in hot-dip galvanizing as the B content increased and the dew point of annealing decreased.

Selective surface oxidation of Si and Mn and the morphology and chemical composition of the oxides were not changed by B addition.

An XPS analysis suggested that BN formation occurred when B was added and annealing was performed at a low dew point, and an experiment showed that the amount of BN had a good correlation with generation of the large bare spot. From these results, B addition is considered to deteriorate coatability in hot-dip galvanizing by causing the formation of BN on the surface when the steel is annealed at a low dew point.

## References

1. Y. Suzuki, Thermodynamic Analysis of Selective Oxidation Behavior of Si and Mn-added Steel during Recrystallization Annealing, *Journal of the Surface Finishing Society of Japan*, **67**, 633 (2016). Doi: <https://doi.org/10.2355/isijinternational.49.564>
2. Y. S. Jin, Development of advanced high strength steels for automotive applications, *La Metallurgia Italiana*, **3**, 43 (2011). <https://www.aimnet.it/allpdf/pdf Pubbl/giu11/jin.pdf>
3. M. Blumenau, A. Barnoush, I. Thomas, H. Hofmann and H. Vehoff, Impact of selective oxidation during inline annealing prior to hot-dip galvanizing on Zn wetting and hydrogen-induced delayed cracking of austenitic FeMnC steel, *Surface and Coatings Technology*, **206**, 542 (2011). Doi: <https://doi.org/10.1016/j.surfcoat.2011.07.081>
4. M. Yoshida, Y. Fushiwaki and S. Taira, Effect of Dew Point on the Selective Surface Oxidation Behavior of Mn Added Steels during Recrystallization Annealing, *Tetsu-to-Hagané*, **108**, 728 (2022). Doi: <https://doi.org/10.2355/tetsutohagane.TETSU-2022-022>
5. L. Cho, S. J. Lee, M. S. Kim, Y. H. Kim, and B. D. Cooman, Influence of Gas Atmosphere Dew Point on the Selective Oxidation and the Reactive Wetting During Hot Dip Galvanizing of CMnSi TRIP Steel, *Metallurgical and Materials Transactions A*, **44A**, 362 (2013). Doi: <https://doi.org/10.1007/s11661-012-1392-1>
6. Y. Okumura, M. Tanaka, Y. Fushiwaki and Y. Nagataki, Influence of Annealing Temperature and Dew Point on Kinetics of Mn External Oxidation, *Tetsu-to-Hagané*, **105**, 676 (2019). Doi: <https://doi.org/10.2355/tetsutohagane.TETSU-2018-153>
7. Y. Suzuki, K. Kyono, C. Kato and K. Mochizuki, Influence of B in Steel on the Morphology of Selectively Formed Mn-oxides on the Steel Sheet Surface during Recrystallization Annealing, *Tetsu-to-Hagané*, **88**, 763 (2002). Doi: [https://doi.org/10.2355/tetsutohagane1955.88.11\\_763](https://doi.org/10.2355/tetsutohagane1955.88.11_763)
8. Y. Suzuki and K. Kyono, Effect of B in Low Carbon Steels on the Si and Mn Selective Surface Oxidation Behavior during Continuous Recrystallization Annealing, *Tetsu-to-Hagané*, **89**, 1158 (2003). Doi: [https://doi.org/10.2355/tetsutohagane1955.89.11\\_1158](https://doi.org/10.2355/tetsutohagane1955.89.11_1158)
9. Z. Ya-long, Z. Ying-yi, Y. Fei-hua, and Z. Zuo-tai, Effect of Alloying Elements (Sb, B) on Recrystallization and Oxidation of Mn-Containing IF Steel, *Journal of Iron and Steel Research International*, **20**, 39 (2013). Doi: [https://doi.org/10.1016/S1006-706X\(13\)60067-9](https://doi.org/10.1016/S1006-706X(13)60067-9)
10. J. F. Moulder, W. F. Stickle, P. E. Sobol and K. D. Bomben, *Handbook of X-ray Photoelectron Spectroscopy*, p. 39, J. Chastain, Perkin-Elmer Corporation, Minnesota (1992).
11. I. Parezanovic, B. Poter and M. Spiegel, B and N Segregation on Dual Phase Steel during Annealing, *Defect and Diffusion Forum*, **237-240**, 934 (2005). Doi: <https://doi.org/10.4028/www.scientific.net/DDF.237-240.934>
12. T. Van De Putte, D. Loison, J. Penning, and S. Claessens, Selective Oxidation of a CMnSi Steel during Heating to 1000 °C: Reversible SiO<sub>2</sub> Oxidation, *Metallurgical and Materials Transactions A*, **39A**, 2875 (2008). Doi: <https://doi.org/10.1007/s11661-008-9636-9>
13. Young-Min Kim and In-Ho Jung, Thermodynamic Evaluation and Optimization of the MnO-B<sub>2</sub>O<sub>3</sub> and MnO-B<sub>2</sub>O<sub>3</sub>-SiO<sub>2</sub> Systems and Its Application to Oxidation of High-Strength Steels Containing Boron, *Metallurgical and Materials Transactions A*, **46A**, 2736 (2015). Doi: <https://doi.org/10.1007/s11661-015-2841-4>